CALCULATION OF ABSORBED DOSE DUE TO THE ⁹⁰Y-DOTATOC PEPTIDE RECEPTOR RADIONUCLIDE THERAPY BY MCNP5/X

by

Marija Ž. JEREMIĆ 1 , Milovan D. MATOVIĆ 1,2 , Suzana B. PANTOVIĆ 3 , Dragoslav R. NIKEZIĆ 4* , and Dragana Ž. KRSTIĆ 4

Department of Nuclear Medicine, Clinical Centre Kragujevac, Kragujevac, Serbia
 Department of Nuclear Medicine, Faculty of Medical Sciences, University of Kragujevac, Kragujevac, Serbia
 Department of Physiology, Faculty of Medical Sciences, University of Kragujevac, Kragujevac, Serbia
 Department of Physics, Faculty of Science, University of Kragujevac, Kragujevac, Serbia

Scientific paper http://doi.org/10.2298/NTRP180411006J

Strong beta emitters, like ⁹⁰Y, ¹⁷⁷Lu labelled peptide, are used for treatment of neuroendocrine tumours where there is a good expression of somatostatin receptors. In this work, MCNP5/X computer software and ORNL human phantoms were used to calculate absorbed dose due to ⁹⁰Y labelled DOTATOC in the peptide receptor radionuclide therapy. Tumour was considered as a sources of beta radiation and represented as a sphere with diameter of 1-4 cm and 5 cm in liver, pancreas, and lungs. Results are expressed as absorbed dose per unit of cumulated activity, S – value in units mGy·(MBq·s)⁻¹. The far largest dose is in tumour itself, then in organ which contains the tumour. Doses in other organs, where the metastasis are the most frequent, due to the bremsstrahlung radiation, are much smaller and could be neglected. The largest dose, 8.66·10⁻³ mGy·(MBq·s)⁻¹ was obtained for tumour with size of 3 cm.

Key words: Monte Carlo simulation, 90 Y-DOTATOC, radionuclide therapy, dosimetry

INTRODUCTION

Peptide receptor radionuclide therapy (PRRT) with radioactive somatostatin analogues was developed recently [1, 2]. It is a targeted molecular therapy based on somatostatin analogues which uses shortlived strong beta emitters like 90Y, 177Lu, or their combination labelled peptide molecules as DOTA-TOC, DOTA-TATE, DOTA-NOC, DOTABOC-ATE etc., [3-9]. It has been recommended to use ⁹⁰Y for tumours larger than 2 cm, and ¹⁷⁷Lu for the treatment of smaller ones, both labelled peptide [10]. This recommendation is based on physical characteristics of ⁹⁰Y, which emits beta particles with the maximal energy of 2.28 MeV, with the range of 11.3 mm in soft tissue. On the other side, 177Lu emits gamma radiation and beta particles with maximal energy of 0.497 MeV, whose range is below 2 mm in tissue [11]. This kind of therapy is standard nowa days in nuclear medicine practice for curing of the neuroendocrine tumours (NET).

The NET do not have specific symptoms, and mainly are diagnosed by the case in later phases of the illness (median, 9.2 years) [12], when numerous metastasis were already spread out through the body. Usually NET appear in gastrointestinal tract, although

The PRRT is applied intravenously and patients spend relatively short period in hospital, up to 3 days. Therapy is usually divided in several portions, where each one is with activity of about 5.5 GBq. Peptide molecules are nephrotoxic [14-16] and relatively large; they could be absorbed in proximal tubules, being retained for long time in renal interstitium [17, 18]. In order to prevent re-absorption of PRRT drugs, positively charged amino acids (like L-Lysine and L-Arginine), which compete for drug transporters, are administered simultaneously [19, 20]. As a consequence, dose delivered to kidney could be large and kidney functions could deteriorate seriously [21]. Some authors proposed to limit the dose in kidney down to 23 Gy [20]. Due to this, it is very important to optimize the dose in pre therapeutic dosimetric study [22-25].

The ⁹⁰Y is very convenient for this kind of therapy because it is a pure beta emitters with maximal energy of 2.28 MeV, the average energy of beta particles is 0.934 MeV and half-life is 64 h. Maximal range of these beta particles in tissue is 11.3 mm [11]. On the other side, it is difficult to detect and measure ⁹⁰Y distribution in human body. This can be done by measuring of bremsstrahlung radiation emitted by beta particles.

The objective of this work is to calculate absorbed dose per one emitted beta particle from ⁹⁰Y, in

they can be found at in other organs in human body [13].

^{*} Corresponding author; e-mail: nikezic@kg.ac.rs

different organs of human body, for various locations and sizes of tumour.

MATERIAL AND METHODS

To perform dose calculation, well known computer software, MCNP5/X [26] was used. Human body is represented with ORNL phantom [27] where organs are given as geometrical bodies filled with various materials. Dose calculations was performed assuming that tumour is spherical in shape with diameter of 1-4 cm and 5 cm, localized in liver, pancreas and lungs, where NET tumours appear most frequently. Tumour was considered as a source of beta particles since up to 30 % of applied activity is deposited and retained in tumour tissue. Such choice of tumour locations was made after 10 years of experience in application of PRRT therapy in Department of Nuclear Medicine in Kragujevac Clinical Centre. The results obtained from MCNP are expressed in MeV g⁻¹ per one emitted particle. Results are later recalculated in mGy/(MBqs).

Tumour locations in patients were determined based on diagnostic OCTREO scan, which was done using Dual Head gamma camera (SIEMENS, HOFFMAN ESTATES, ILLINOIS, USA), with low energy — high resolution collimators, in matrix 256 1024 pixels, with the table speed 5 cm/min. This is the standard procedure for patients with NET illness. Totally 740 MBq of ^{99m}Tc-Tectrodyd produced by POLATOM, Poland, was applied intravenously in a single dose.

Figure 1 shows images of human body obtained by gamma camera and longitudinal cross-section view of corresponding ORNL phantoms (on the left side of gamma camera images).

Monte Carlo simulations were carried out for the following organs: liver, pancreas and lungs, as well as the central area of the abdomen, where the tumour was assumed:

The liver (volume is 1830 cm³) is given as an elliptical cylinder

$$\frac{x}{a} = \frac{y}{b} = 1 \tag{1}$$

intersected with a plane

$$\frac{x}{x_{\rm m}} \frac{y}{y_{\rm m}} \frac{z}{z_{\rm m}} \quad 1 \quad \text{and} \quad z_1 \quad z \quad z_{\rm m} \quad (2)$$

Parameters a and b are 16.50 and 8, respectively. Values for $x_{\rm m}$, $y_{\rm m}$, and $z_{\rm m}$ are: 35, 45, and 43, respectively (all in cm).

The pancreas is an ellipsoid with a section removed and defined by

$$\frac{x + x_0}{a} = \frac{y}{b} = \frac{z + z_0}{c} = 1$$
 and $x + x_0$ (3)

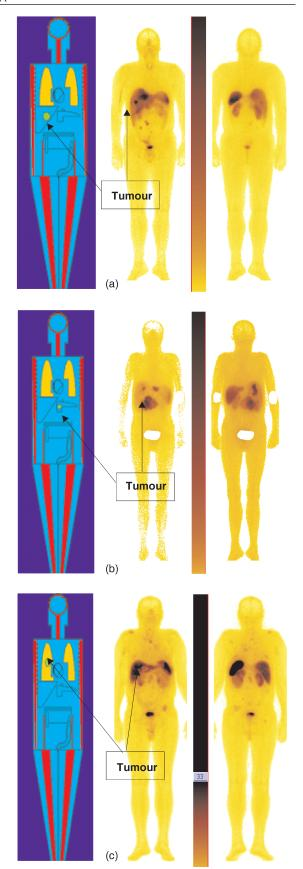


Figure 1. The images of whole body scintigraphy in AP, and PA projection, of three patients with NET tumours in (a) liver, (b) pancreas, and (c) right lung lobe. Left of scintillation images, the graphical output from MCNP code with ORNL phantom are shown, with the tumour locations used in calculations

where parameters x_0 , z_0 , x_1 , a, b, and c are: -1, 37, 3, 16, 1.20, and 3.30 (in cm), respectively.

Each lungs lobe is represented as a half ellipsoid, where upper part is removed. The lungs (volume is 1810 cm³ for right, and 1560 cm³ for left lung) are defined as

$$\frac{x \quad x_0}{a} \quad \frac{z}{v} \quad \frac{z}{v} \quad \frac{z \quad z_0}{c} \quad 1 \text{ and } z \quad z_0 \quad (4)$$

If $z_{1R,L}$ z $z_{2R,L}$ and y $y_{1R,L}$, x $x_{1R,L}$. The letters R and L refer to the right and left lungs. The appropriate values (in cm) for x_0 , z_0 , x_{1R} , x_{1L} , y_{1R} , y_{1L} , z_{1R} , z_{2R} , z_{2L} , a, b, and c are: 8.50, 43.50, -5.40, 8, 1.50, 1, 46, 54, 55, 5, 7.50, and 24, respectively.

According to ORNL, human phantom consists of three types of tissues, skeletal, lung and soft, with different densities and elemental compositions. All equations for organs of ORNL phantom, with other relevant information (chemical compositions, volumes, masses *etc.*), were programmed in input files for MCNP code [28]. By combining surfaces through Bull algebra, MCNP forms cells, representing various organs.

To calculate the mean absorbed doses in other organs, when the source of radiation is located in the tumour, ORNL phantom of human body was also used. This model does not give details of human kidneys, liver and tumour. In addition, uniform distribution of activity in these organs is assumed. The dose in other organs originated from bremsstrahlung radiation, emitted by beta particles in tumour.

Since the kidneys appear in pair, they are presented in MCNP as the union of regions which contain left and right kidney. The number on histories must be increased to ensure low statistical error. As the calculation time in this case would be enormous, calculations were done separately.

For the calculations, a spectrum of electrons emitted by 90 Y is needed. Continuous spectrum of beta (β) radiation emitted by 90 Y was taken from reference [29]. Particle energy was sampled according to yields using random method incorporated in MCNP software. In order to simulate emission of whole spectrum of β^- radiation, large number of histories was created (10^8) , to ensure uncertainty lower than few percent. As a result of computation, the F6 MCNP tally produces the output in MeVg⁻¹ per particle, which was recalculated in the absorbed dose in Gy in targeted organs, per one emitted (β) particle of radiation from the source, i. e. from the tumour in this case.

Since the yields for beta emission of 90 Y is equal to $0.9982 \sim 1$, results obtained by MCNP calculations can be expressed as absorbed dose per unit cumulated activity, S – value (mGy(MBqs)⁻¹) [30], which is the most often used units in literature in this field

$$S(k \quad h) \quad \Delta_{i} \Phi(k \quad h)$$
 (5)

where k is a target organ and h is a source organ, $\Delta_i = n_i E_i$ and E_i is the energy emitted for radiation type i

with probability n_i , a (k h) is specific absorbed fraction (SAF) defined as the ratio of the absorbed fraction divided by the mass of target organ m_k

$$\Phi(k - h) = \frac{\phi(k - h)}{m_k} \tag{6}$$

 $\phi(k - h)$ is the absorbed fraction (AF) given as

$$\phi(k - h) = \frac{E}{E_0} \tag{7}$$

the ratio of the energy, E, absorbed in target region k, to the energy E_0 emitted in source region h.

RESULTS AND DISCUSSION

Results are presented in tabs. 1-3. The S-values in organs of human body, assuming that source is in liver, pancreas and lung, respectively. As it was previously written, calculation was performed for the beta spectrum of ⁹⁰Y. Dependence of S-value on tumour size is also shown in fig. 2.

Location of the tumour/source was chosen to fit the images obtained from the real patients who were treated with this therapy (see fig. 1). Post therapeutic scintigraphy is not performed in practice because ⁹⁰Y is almost pure beta emitter. It is possible to obtain bremsstrahlung scintigraphy, but it does not satisfy criteria for quantitative estimation of distribution of ⁹⁰Y-DOTATOC [31]. Due to this reason, pre therapeutic prediction of ⁹⁰Y distribution in human body is often conducted with radiopharmaceutical with similar bio kinetic [32]. Nevertheless, in some publications bremsstrahlung scintigraphy was used to measure ⁹⁰Y distribution [33].

By inspection of tabs. 1-3 it is seen that doses are dependent on the tumour diameter. Doses in tumour decreases with its size. This is due to the increasing of tumour volume and mass with the r^3 , while the tumour surface increases with r^2 , where r is the tumour radius. In this way, fraction of beta particles which escape from the tumour decreases with the tumour size, but the mass of the tumour increases with r^3 .

In tab. 1 doses are given when the tumour is in liver. The largest doses are in gall bladder and adrenals

In tab. 2 doses are given for the tumour in pancreas. Again, doses are larger in pancreas and adrenals than in other organs.

In tab. 3 results are given for the tumour in lung. Here doses in adrenals are much smaller, while the thyroid and stomach are larger than in previous cases.

However, doses in tumour do not depend on distribution of ⁹⁰Y within the tumour. Similar finding was observed in ref. [34].

In organs where the tumour is located, dose is larger 4 to 5 order of magnitude than in other organs. As it was expected, doses are larger in organs closer to

Table 1. The S-values in mGy/(MBqs) to the target k per unit cumulated activity in the source region k for different tumour size when the tumour is in the liver. Comparison with Stabin *et al.* [35]

Organs	Diameter 1 cm	Stabin <i>et al.</i> [35] for point source	Diameter 2 cm	Diameter 3 cm	Diameter 4 cm	Diameter 5 cm
Adrenals	$0.20 \cdot 10^{-7}$	$0.28 \cdot 10^{-7}$	$0.20 \cdot 10^{-7}$	$0.20 \cdot 10^{-7}$	$0.21 \cdot 10^{-7}$	$0.21 \cdot 10^{-7}$
Bladder	$0.45 \cdot 10^{-9}$	$0.95 \cdot 10^{-9}$	$0.49 \cdot 10^{-9}$	$0.49 \cdot 10^{-9}$	$0.49 \cdot 10^{-9}$	$0.48 \cdot 10^{-9}$
Bone surface	$0.29 \cdot 10^{-8}$	$0.66 \cdot 10^{-8}$	$0.29 \cdot 10^{-8}$	$0.29 \cdot 10^{-8}$	$0.3 \cdot 10^{-8}$	0.3 · 10 ⁻⁸
Stomach	$0.42 \cdot 10^{-8}$	$0.91 \cdot 10^{-8}$	$0.42 \cdot 10^{-8}$	$0.42 \cdot 10^{-8}$	$0.43 \cdot 10^{-8}$	$0.42 \cdot 10^{-8}$
Small intestine	$0.39 \cdot 10^{-8}$	$0.71 \cdot 10^{-8}$	$0.38 \cdot 10^{-8}$	$0.38 \cdot 10^{-8}$	$0.39 \cdot 10^{-8}$	$0.39 \cdot 10^{-8}$
Colon	$0.36 \cdot 10^{-8}$	_	$0.36 \cdot 10^{-8}$	$0.36 \cdot 10^{-8}$	$0.36 \cdot 10^{-8}$	$0.37 \cdot 10^{-8}$
Gall bladder	$0.35 \cdot 10^{-7}$	$0.58 \cdot 10^{-7}$	$0.35 \cdot 10^{-7}$	$0.35 \cdot 10^{-7}$	$0.35 \cdot 10^{-7}$	$0.36 \cdot 10^{-7}$
Kidneys	$0.18 \cdot 10^{-7}$	$0.18 \cdot 10^{-7}$	$0.18 \cdot 10^{-7}$	$0.18 \cdot 10^{-7}$	$0.18 \cdot 10^{-7}$	$0.18 \cdot 10^{-7}$
Liver	$0.32 \cdot 10^{-4}$	$0.17 \cdot 10^{-6}$	$0.17 \cdot 10^{-4}$	$0.11 \cdot 10^{-4}$	$0.87 \cdot 10^{-5}$	$0.67 \cdot 10^{-5}$
Lungs	$0.64 \cdot 10^{-8}$	$0.13 \cdot 10^{-7}$	$0.64 \cdot 10^{-8}$	$0.64 \cdot 10^{-8}$	$0.65 \cdot 10^{-8}$	$0.65 \cdot 10^{-8}$
Pancreas	$0.14 \cdot 10^{-7}$	$0.23 \cdot 10^{-7}$	$0.14 \cdot 10^{-7}$	$0.14 \cdot 10^{-7}$	$0.14 \cdot 10^{-7}$	$0.14 \cdot 10^{-7}$
Spleen	$0.25 \cdot 10^{-8}$	$0.44 \cdot 10^{-8}$	$0.25 \cdot 10^{-8}$	$0.24 \cdot 10^{-8}$	$0.25 \cdot 10^{-8}$	$0.25 \cdot 10^{-8}$
Thyroid	$0.07 \cdot 10^{-9}$	$0.66 \cdot 10^{-9}$	$0.15 \cdot 10^{-9}$	$0.12 \cdot 10^{-9}$	$0.14 \cdot 10^{-9}$	$0.17 \cdot 10^{-9}$
Tumour	0.16	_	$2.68 \cdot 10^{-2}$	$8.66 \cdot 10^{-3}$	$3.81 \cdot 10^{-3}$	$2.0 \cdot 10^{-3}$

Table 2. The S – values in mGy/(MBqs) to the target k per unit cumulated activity in the source region k for different tumour size when the tumour is in the pancreas

Organs	Diameter 1 cm	Diameter 2 cm	Diameter 3 cm	Diameter 4 cm	Diameter 5 cm
Adrenals	$0.47 \cdot 10^{-7}$	0. 46·10 ⁻⁷	$0.47 \cdot 10^{-7}$	$0.48 \cdot 10^{-7}$	$0.49 \cdot 10^{-7}$
Bladder	$0.58 \cdot 10^{-9}$	$0.56 \cdot 10^{-9}$	$0.55 \cdot 10^{-9}$	$0.61 \cdot 10^{-9}$	$0.60 \cdot 10^{-9}$
Bone surface	$0.44 \cdot 10^{-8}$	$0.45 \cdot 10^{-8}$	$0.45 \cdot 10^{-8}$	$0.45 \cdot 10^{-8}$	$0.47 \cdot 10^{-8}$
Stomach	$0.29 \cdot 10^{-7}$	$0.29 \cdot 10^{-7}$	$0.29 \cdot 10^{-7}$	$0.29 \cdot 10^{-7}$	$0.30 \cdot 10^{-7}$
Small intestine	$0.51 \cdot 10^{-8}$	$0.51 \cdot 10^{-8}$	$0.51 \cdot 10^{-8}$	$0.51 \cdot 10^{-8}$	$0.51 \cdot 10^{-8}$
Colon	$0.43 \cdot 10^{-8}$	$0.43 \cdot 10^{-8}$	$0.44 \cdot 10^{-8}$	$0.42 \cdot 10^{-8}$	$0.43 \cdot 10^{-8}$
Gall bladder	$0.36 \cdot 10^{-7}$	$0.34 \cdot 10^{-7}$	$0.37 \cdot 10^{-7}$	$0.36 \cdot 10^{-7}$	$0.38 \cdot 10^{-7}$
Kidneys	$0.19 \cdot 10^{-7}$	$0.18 \cdot 10^{-7}$	$0.19 \cdot 10^{-7}$	$0.19 \cdot 10^{-7}$	$0.19 \cdot 10^{-7}$
Liver	$0.18 \cdot 10^{-7}$	$0.18 \cdot 10^{-7}$	$0.19 \cdot 10^{-7}$	$0.19 \cdot 10^{-7}$	$0.19 \cdot 10^{-7}$
Lungs	$0.52 \cdot 10^{-8}$	$0.53 \cdot 10^{-8}$	$0.53 \cdot 10^{-8}$	$0.52 \cdot 10^{-8}$	$0.53 \cdot 10^{-8}$
Pancreas	$0.65 \cdot 10^{-3}$	$0.33 \cdot 10^{-3}$	$0.16 \cdot 10^{-3}$	$0.79 \cdot 10^{-4}$	$0.33 \cdot 10^{-4}$
Spleen	$0.16 \cdot 10^{-7}$	$0.16 \cdot 10^{-7}$	$0.16 \cdot 10^{-7}$	$0.16 \cdot 10^{-7}$	$0.16 \cdot 10^{-7}$
Thyroid	$0.12 \cdot 10^{-9}$	$0.14 \cdot 10^{-9}$	$0.12 \cdot 10^{-9}$	$0.02 \cdot 10^{-9}$	$0.08 \cdot 10^{-9}$
Tumour	0.16	$2.68 \cdot 10^{-2}$	$8.66 \cdot 10^{-3}$	$3.81 \cdot 10^{-3}$	$2.0 \cdot 10^{-3}$

Table 3. The S – values in mGy/(MBqs) to the target k per unit cumulated activity in the source region k for different tumour sizes when the tumour is at the lung

unicient tumour sizes when the tumour is at the rung						
Organs	Diameter 1 cm	Diameter 2 cm	Diameter 3 cm	Diameter 4 cm	Diameter 5 cm	
Adrenals	$0.47 \cdot 10^{-8}$	$0.45 \cdot 10^{-8}$	$0.47 \cdot 10^{-8}$	$0.45 \cdot 10^{-8}$	$0.43 \cdot 10^{-8}$	
Bladder	$0.70 \cdot 10^{-10}$	$0.75 \cdot 10^{-10}$	$0.82 \cdot 10^{-10}$	$0.86 \cdot 10^{-10}$	$0.68 \cdot 10^{-10}$	
Bone surface	$0.41 \cdot 10^{-8}$	$0.41 \cdot 10^{-8}$	$0.40 \cdot 10^{-8}$	$0.40 \cdot 10^{-8}$	$0.39 \cdot 10^{-8}$	
Stomach	$0.12 \cdot 10^{-8}$	$0.12 \cdot 10^{-8}$	$0.12 \cdot 10^{-8}$	$0.12 \cdot 10^{-8}$	$0.12 \cdot 10^{-8}$	
Small intestine	$0.41 \cdot 10^{-9}$	$0.40 \cdot 10^{-9}$	$0.41 \cdot 10^{-9}$	$0.39 \cdot 10^{-9}$	$0.39 \cdot 10^{-9}$	
Colon	$0.36 \cdot 10^{-9}$	$0.35 \cdot 10^{-9}$	$0.35 \cdot 10^{-9}$	$0.34 \cdot 10^{-9}$	$0.35 \cdot 10^{-9}$	
Gall bladder	$0.20 \cdot 10^{-8}$	$0.18 \cdot 10^{-8}$	$0.20 \cdot 10^{-8}$	$0.19 \cdot 10^{-8}$	$0.19 \cdot 10^{-8}$	
Kidneys	$0.15 \cdot 10^{-8}$	$0.15 \cdot 10^{-8}$	$0.15 \cdot 10^{-8}$	$0.15 \cdot 10^{-8}$	$0.15 \cdot 10^{-8}$	
Liver	$0.60 \cdot 10^{-8}$	$0.59 \cdot 10^{-8}$	$0.58 \cdot 10^{-8}$	$0.58 \cdot 10^{-8}$	$0.57 \cdot 10^{-8}$	
Lungs	$0.63 \cdot 10^{-4}$	$0.33 \cdot 10^{-4}$	$0.22 \cdot 10^{-4}$	$0.17 \cdot 10^{-4}$	$0.13 \cdot 10^{-4}$	
Pancreas	$0.25 \cdot 10^{-8}$	$0.27 \cdot 10^{-8}$	$0.25 \cdot 10^{-8}$	$0.25 \cdot 10^{-8}$	$0.26 \cdot 10^{-8}$	
Spleen	$0.11 \cdot 10^{-8}$	$0.11 \cdot 10^{-8}$	$0.11 \cdot 10^{-8}$	$0.10 \cdot 10^{-8}$	$0.11 \cdot 10^{-8}$	
Thyroid	$0.12 \cdot 10^{-8}$	$0.12 \cdot 10^{-8}$	$0.98 \cdot 10^{-9}$	$0.11 \cdot 10^{-8}$	$0.11 \cdot 10^{-8}$	
Tumour	0.16	2.66 · 10 ⁻²	$8.62 \cdot 10^{-3}$	$3.80 \cdot 10^{-3}$	$1.99 \cdot 10^{-3}$	

the tumour than in other distal organs. Similar values were published in [35]. Stabin *et al.* [35] calculated absorbed dose from point like 90 Y source at the distance of 3 cm as $1.61\cdot10^{-4}$ GyMBq $^{-1}$, while in this

work value 8.66·10⁻³ mGy(MBqs)⁻¹, was found. However, in this work calculation was performed for spherical source while Stabin *et al.* [35] used point source, so, the results are not directly comparable.

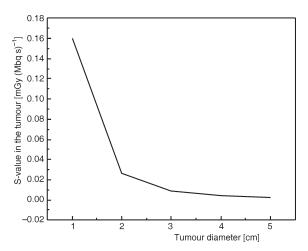


Figure 2. Dependence of absorbed dose per unit cumulated activity (S-value) on the tumour size

Nevertheless, comparison with Stabin *et al.* [35] is given in third column in tab. 1. Comparison shows that the same order of magnitude is in all organs, but the difference is smaller for distal organs, and larger for organs closer to the source. Ahangari *et al.* [36], also calculated dose from various sizes of spherical sources but, the results again are not directly comparable.

Calculations performed here – were done with 10^8 simulations in order to obtain results with statistical uncertainty smaller than 1 %. Other uncertainties are possible due to variability of size of human body, tissue density and its chemical composition, *etc*.

CONCLUSION

Absorbed dose per unit exposure, *i. e.*, S-value in mGy/(MBqs) from ⁹⁰Y, in different organs of human body, were calculated in this work. As expectable, doses are largest in tumour and in organ where the tumour is situated. In addition, doses are larger in organs near the tumour and much smaller in distant organs where they could be neglected. In addition, doses in organs out of tumour weakly depend on tumour size.

According to European directive 2013/59/, there is a need for estimation of absorbed doses in all medical exposure of ionizing radiation [37]. Since there is no bio kinetic model for ⁹⁰Y recommended by the ICRP, it is necessary to develop such model where the previously given results of S-values could be used for dose assessment.

ACKNOWLEDGMENT

The present work was supported by the Ministry of Education, Science and Technological Development of Serbia, through the project No 171021.

AUTHOR'S CONTRIBUTIONS

Conceived and designed the computations: M. Ž. Jeremić and D. Ž. Krstić. Performed the computations: D. Ž. Krstić. Analyzed the data: all authors. Wrote the paper: D. R. Nikezić, M. Ž. Jeremić, and D. Ž. Krstić. All the authors participated in the discussion of the results presented in the final version of the manuscript.

REFERENCES

- [1] Severo, S., et al., Peptide Receptor Radionuclide Therapy in the Management of Gastrointestinal Neuroendocrine Tumors: Efficacy Profile, Safety, and Quality of Life, Onco Targets and Therapy, 10 (2017), Jan., pp. 551-557
- [2] Bison, S. M., et al., Peptide Receptor Radionuclide Therapy Using Radiolabelled Somatostatin Analogs: Focus on Future Developments, Clin. Transl. Imaging, 2 (2014), 1, pp. 55-66
- [3] De. Jong, M., et al., Pre-Clinical Comparison of [DTPA0, Tyr3]Octreotide and [DOTA0, D-Phe1, Tyr3] Octreotide as Carriers for Somatostatin Receptor-Targeted Scintigraphy and Radionuclide Therapy, Int. J. Cancer, 75 (1998), Jan., pp. 406-11
- [4] Bodei, L., et al., Radionuclide Therapy with Iodine-125 and Other Auger-Electron-Emitting Radionuclides: Experimental Models and Clinical Applications, Cancer Biother. Radiopharm., 18 (2003), 6, pp. 861-877
- [5] Cescato, R., et al., Internalization of sst2, sst3, and sst5receptors: Effects of Somatostatin Agonists and Antagonists, J. Nucl. Med., 47 (2006), 3, pp. 502-511
- [6] Reubi, J. C., et al., Candidates for Peptide Receptor Radiotherapy Today and in the Future, J. Nucl. Med., 46 (2005), Jan., pp. 67S-75S
- [7] de Jong, M., et al., Radiolabelled Peptides for Tumour Therapy: Current Status and Future Directions, Plenary lecture at the EANM 2002, Eur. J. Nucl. Med. Mol. Imaging, 30 (2003), 3, pp. 463-469
- [8] Virgolini, I., et al., New Trends in Peptide Receptor Radioligandsradio Ligands, Q. J. Nucl. Med., 45 (2001), 2, pp. 153-159
- [9] van der Hoek, J., et al., Novel Subtype Specific and Universal Somatostatin Analogues: Clinical Potential and Pitfalls, Curr. Pharm. Des., 11 (2005), 12, pp. 1573-1592
- [10] Bodei, L., et al., The Joint IAEA, EANM, and SNMMI Practical Guidance on Peptide Receptor Radionuclide Therapy (PRRNT) in Neuroendocrine Tumours, Eur. J. Nucl. Med. Mol. Imaging, 40 (2013), 5, pp. 800-816
- [11] Cremonesi, M., et al., Dosimetry in Peptide Radionuclide Receptor Therapy: A Review, J. Nucl. Med., 47 (2006), Sept., pp. 1467-1475
- [12] Singh, S., et al., Patient-Reported Burden of a Neuroendocrine Tumour (NET) Diagnosis: Results from the First Global Survey of Patients with NET, J.G.O. 3 (2017), 1, pp. 43-53
- [13] Matovic, M., Peptide receptor Radionuclide Therapy of Neuroendocrine Tumors: Case Series, Arch. Oncol., 20 (2012), 3-4, pp. 143-148
- [14] Bodei, L., et al., Long-Term Evaluation of Renal Toxicity After Peptide Receptor Radionuclide Therapy with 90Y-DOTATOC and 177Lu-DOTATATE: the Role of Associated Risk Factors, Eur. J. Nucl. Med. Mol. Imaging 35 (2008), Oct., pp. 1847-1856

- [15] Bodei, L., et al., Long-Term Tolerability of PRRT in 807 Patients with Neuroendocrine Tumours: the Value and Limitations of Clinical Factors, Eur. J. Nucl. Med. Mol. Imaging, 42 (2015), pp. 5-19

 [16] Guerriero, F., et al., Kidney Dosimetry in ¹⁷⁷Lu and ⁹⁰Y
- Peptide Receptor Radionuclide Therapy: Influence of Image Timing, Time-Activity Integration Method, and Risk Factors, Biomed. Res. Int., 2013 (2013), p. 12
- Vegt, E., et al., Renal Toxicity of Radiolabelled Peptides and Antibody Fragments: Mechanisms, Impact on Radionuclide Therapy, and Strategies for Prevention, *J. Nucl. Med.*, *51* (2010), 7, pp. 1049-1058
- [18] Imhof, A., et al., Response, Survival, and Long-Term Toxicity After Therapy with the Radiolabeled Somatostatin Analogue [90Y-DOTA]-TOC in Metastasized Neuroendocrine Cancers, J. Clin. Oncol., 29 (2011), Jun., pp. 2416-2423
- Rolleman, E. J., et al., Safe and Effective Inhibition of Renal Uptake of Radiolabelled Octreotide by a Combination of Lysine and Arginine, Eur. J. Nucl. Med. Mol. Imaging, 30 (2003), 1, pp. 9-15
- [20] Bergsma, H., et al., Nephrotoxicity After PRRT with (177)Lu-DOTA-Octreotate, Eur. J. Nucl. Med. Mol. Imaging, 43 (2016), 10, pp. 1802-1811
- [21] Živković, M., et al., Influence of Electromagnetic and Nuclear Radiationin Medicine for Therapy and Diagnosis Through Processes, Facts and Statistical Analysis, Nucl Technol Radiat, 32 (2017), 1, pp. 91-98
- [22] Hardiansyah, D., et al., Prediction of Time-Integrated Activity Coefficients in PRRT Using Simulated Dynamic PET and a Pharmacokinetic Model, Phys. Med., 42 (2017), July, pp. 298-304
- [23] Kletting, P., et al., Optimized Peptide Amount and Activity for ⁹⁰Y-LabeledDOTATATE Therapy, J. Nucl. Med., 57 (2016), 4, pp. 503-508
- [24] Hindorf, C., et al., Dosimetry for 90Y-DOTATOC Therapies in Patients with Neuroendocrine Tumors, Cancer Biother. Radiopharm., 22 (2007), Feb., pp.
- [25] Oksuza, M. O., et al., Peptide Receptor Radionuclide Therapy of Neuroendocrine Tumors ⁹⁰Y-DOTATOC: Is Treatment Response Predictable by Pre-Therapeutic Uptake of 68Ga-DOTATOC?, Diagn. Interv. Imaging, 95 (2014), Mar., pp. 289-300
- [26] ***, X-5 Monte Carlo Team. MCNP-a General Monte Carlo N-Particle Transport Code, Version 5 Vol. I:

- Overview and Theory Los Alamos, NM: Los Alamos National Laboratory; LA- UR- 03- 1987, 2003
- Eckerman, K. F., et al., The ORNL Mathematical Phantom Series. Oak Ridge National Laboratory Report (1996) Oak Ridge, TN, USA, Update do April 2000 2009, http://ordose.ornl.gov/resources/Mird.pdf
- [28] Krstić, D., Nikezić, D., Input Files with ORNL-Mathematical Phantoms of the Human Body for MCNP-4B, Com. Phys. Commun., 176 (2007), Jan., pp. 33-37
- ***. Table of Radioactive Isotopes, http:// nucleardata.nuclear.lu.se/toi/perchart.htm
- Villoing, D., et al., Internal Dosimetry with the Monte Carlo code GATE: Validation Using the ICRP/ICRU Female Reference Computational Model, Phys. Med. Biol., 62 (2017), Mar., pp. 1885-1904
- [31] Minarik, D., et al., Evaluation of Quantitative Planar Y Bremsstrahlung Whole-Body Imaging, *Phys.* Med. Biol., 54 (2009), Oct., pp. 5873-5883
- [32] Brans, B., et al., Clinical Radionuclide Therapy Do-
- imetry: the Quest for the "Holy Gray", Eur. J. Nucl. Med. Mol. Imaging., 34 (2012), 5, pp. 772-786

 [33] Menda, Y., et al., "90Y-DOTATOC Dosimetry-Based Personalized Peptide Receptor Radionuclide Therapy J. Nucl. Med. Building to the Control of the Personalized Peptide Receptor Radionuclide Therapy J. Nucl. Med. Building to the Control of the Personalized Peptide Receptor Radionuclide Therapy J. Nucl. Med. Building to the Control of the Personalized Peptide Receptor Radionuclide Therapy J. Nucl. Med. Building to the Personalized Peptide Receptor Radionuclide Therapy J. Nucl. Med. Building to the Personalized Peptide Receptor Radionuclide Therapy Dosimetry: The Personalized Peptide Receptor Radionuclide Therapy Dosimetry States and Personalized Peptide Receptor Radionuclide Therapy Dosimetry States and Personalized Peptide Receptor Radionuclide Therapy Dosimetry Radionuclide Therapy R apy, J. Nucl. Med. Published on March 9, 2018, as doi:10.2967/jnumed.117.202903 [Epub ahead of
- Konijnenberg, W. M., et al., A Stylized Computational Model of the Rat for Organ Dosimetry in Support of Preclinical Evaluations of Peptide Receptor Radionuclide Therapy with ⁹⁰Y, ¹¹¹In, or ¹⁷⁷Lu, *J. Nucl. Med.*, 45 (2004), Jul., pp. 1260-1269
- [35] Stabin, M. G., et al., Bremsstrahlung Radiation Dose in Yttrium-90 Therapy Applications, *J. Nucl. Med.*, *35* (1994), 8, pp. 1377-1380
- [36] Ahangari, H. T., et al., Evaluation of MCNPX and GATE with HotSpot for Internal Dosimetry (Simulation Study), *Int. J. Adv. Biol. Biom. Res.*, 3 (2015), Sept., pp. 275-284
- ***, COUNCIL DIRECTIVE 2013/59/EURATOM of 5 December 2013 Laying Down Basic Safety Standards for Protection Against the Dangers Arising from Exposure to ionising Radiation, and Repealing Directives 89/618/Euratom, 90/641/Euratom, 96/29/ Euratom, 97/43/Euratom and 2003/122/Euratom, 2014, Official Journal of the European Union

Received on April 11, 2018 Accepted on October 1, 2018

Марија Ж. ЈЕРЕМИЋ, Милован Д. МАТОВИЋ, Сузана Б. ПАНТОВИЋ, Драгослав Р. НИКЕЗИЋ, Драгана Ж. КРСТИЋ

РАЧУНАЊЕ АПСОРБОВАНЕ ДОЗЕ ПРИ 90 Y-DOTATOC ПЕПТИДНОЈ **РАДИОНУКЛИДНОЈ ТЕРАПИЈИ, ПОМОЋУ** MCNP5/X

Пептиди (DOTATOC, DOTATATE) обележени јаким бета емитерима, као што су 90 Y и 177 Lu, користе се у терапији неуроендокриних тумора који имају јак афинитет за соматостатинске рецепторе. У овом раду коришћени су MCNP5/X софтвер и ORNL фантоми људског тела, за рачунање апсорбованих доза услед примене ⁹⁰Y-DOTATOC. Тумори су разматрани као извор бета зрачења и представљени су у облику сфера дијаметара 1-4 ст и 5 ст у јетри, панкреасу и плућима. Резултати су изражени у облику апсорбоване дозе по јединици кумулативне активности, S-вредност у јединицама (mGy·(MBqs)⁻¹). Највећа доза је у самом тумору, мања је у органу у коме се тумор налази али није занемарљива. Дозе у осталим оганима, које потичу од закочног зрачења су далеко мање и могу се занемарити. Максимална доза је добијена за пречник тумора од 3 cm, $8.66\ 10^{-3}\ mGy\ (MBqs)^{-1}$, док је за остале пречнике тумора добијена мања вредност.